

Combined approach for site investigation in terms of the analysis of rainfall induced landslides

Une approche combiné pour l'investigation d'un site pour l'analyse de glissements causés par l'infiltration de pluie

A. Thielen, S. Friedel, M. Plötze, S. M. Springman

Institute for Geotechnical Engineering, Swiss Federal Institute of Technology, ETH Zurich

ABSTRACT

The risk of surficial landslide events arising increases wherever the combination of intense periods of rainfall, steep topography and soil conditions are critical. Monitoring of the condition of the ground can provide valuable information for the risk assessment of potential landslides. Prior to installing the instruments, a detailed site investigation is essential. Ideally, both monitoring and initial site investigation should deliver high-resolution 3D spatial information about the soil conditions without creating disturbance such as artificial paths of infiltration. An integrated investigation of a test site is presented. Results of geological, geophysical and geotechnical methods are compared and used to derive an integrated model. In addition to geological studies and classical geotechnical testing including dynamic penetration tests and analysis of soil samples, a geophysical investigation was carried out using electrical resistivity tomography. The integrated model of the subsurface resulting from several complementary datasets suggests that this procedure is very useful for optimising the design of a monitoring system, in terms of quality, cost efficiency and predictive capability of the hydro-mechanical models derived from, or validated by, the planned monitoring system for areas likely to be subject to landslides.

RÉSUMÉ

Le risque de glissements de terrain superficiels augmente si la combinaison d'une période de précipitations intenses, d'une topographie raide et des conditions de sol est critique. La surveillance de l'état du sous-sol peut donner des informations utiles pour l'estimation des risques de glissements. Avant l'installation des instruments, il est essentiel de procéder à une prospection détaillée du site. Dans le meilleur des cas, la surveillance et la prospection du site donnent des informations 3-dimensionnelles sans perturber l'état du terrain. L'investigation intégrée d'un site est présentée dans ce travail. Les résultats de méthodes géologiques, géophysiques et géotechniques sont comparés et utilisés pour dériver un modèle intégré. En plus des études géologiques et des essais géotechniques classiques y compris des essais dynamiques de pénétration et l'analyse d'échantillons de sol, une étude géophysique utilisant la tomographie électrique de résistivité a été exécutée. Le modèle intégré obtenu à partir de plusieurs ensembles de données complémentaires suggère que ce procédé permet d'optimiser la conception d'un système de surveillance en terme de qualité, d'efficacité économique et de capacité prédictive des modèles hydro-mécaniques dérivés du système de surveillance prévu pour les zones susceptibles de subir des glissements de terrain.

1 INTRODUCTION

Steep slopes with an inclination greater than the friction angle of the soil can be stable due to the effect of suction, which augments the shear resistance and can be represented as an apparent cohesion. When rainfall starts to saturate the soil, suction reduces and the following reduction of shear resistance can result in failure at worst, culminating in a landslide or debris flow.

A series of 42 landslides occurred in May 2002 in North Switzerland near the river Rhine after an extreme event, in which 100 mm rain fell in 40 minutes (Fischer et al., 2003). The location of 6 examples is plotted in Figure 1 with a star.

To investigate the dependence between rainfall, suction, saturation and shear resistance, a test site with similar geology, topography and topsoil structure has been chosen in this endangered area beside the river Rhine (Fig. 1 & Fig. 2). The grass covered site is characterised by an average slope angle of 27° and shallow quaternary sediments overlying a sandstone basement (Fig. 3). It has been equipped with various measuring devices to obtain meteorological data, infiltration and outflow. For the observation of suction and moisture content for a period of one year, Tensiometers, TDRs (time domain reflectometers) and Moisture Point (ESI, 2004) devices have been installed.

The results of a comprehensive site investigation prior to the installation of the instrumentation are reported. It yielded a high resolution model of the subsurface to optimise the placement of sensors for the monitoring experiment.

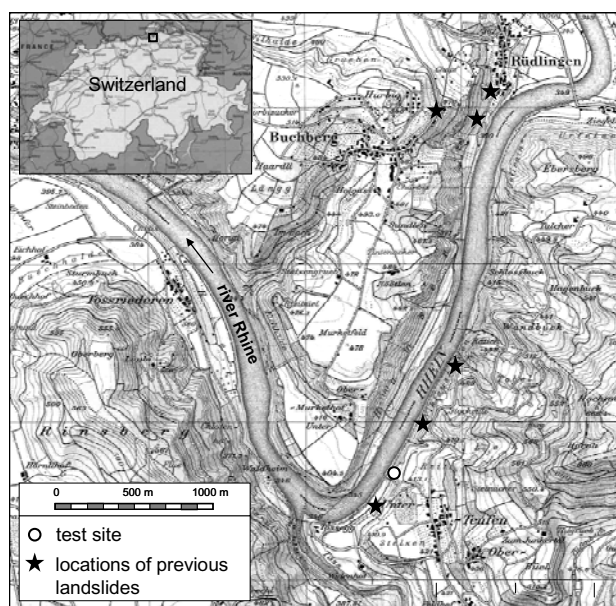


Figure 1. Geographical location of the test site and of previous landslides from the May 2002 event (after Bundesamt für Landestopographie, 1976 (detailed map); University of Texas Libraries, 2000 (map of Switzerland)).

2 SITE INVESTIGATION

The investigation had to be non-destructive, cost efficient and should deliver 3-dimensional information about the ground conditions in the area of the test site. A combination of geophysical, geological and geotechnical methods was applied.

2.1 Geology

The geological map (Hantke, 1967) of the area was studied in detail during a visual site inspection. Samples have been taken in a steep cutting caused by a stream about 50 m from the test field and analysed in terms of mineralogy. As a result, assumptions could be made about the bedding of the underlying rock inside the slope (Fig. 3): sandstone deposited under saltwater in the lower part of the field is overlaid by a denser 2m thick layer of upper freshwater sandstone and in the upper part of the field by quaternary deposits.

2.2 Geotechnical investigation

The geotechnical investigation included 13 dynamic penetration tests and sampling at 15 locations using rammed samplers, hand augers and a rotary drilling device (Fig. 2). The dynamic penetration tests were carried out to detect the surface of the sandstone.

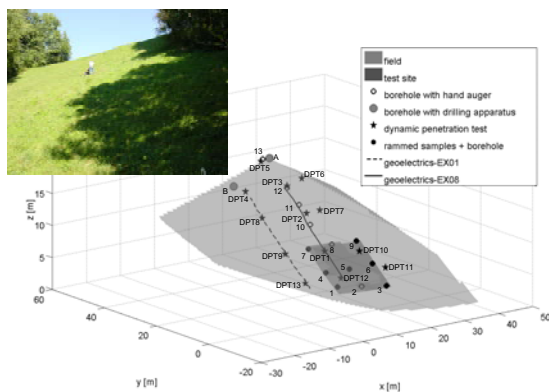


Figure 2. Location of the test site, geotechnical investigation points (rammed samples, dynamic penetration tests, boreholes and two of the geoelectrical ERT-profiles).

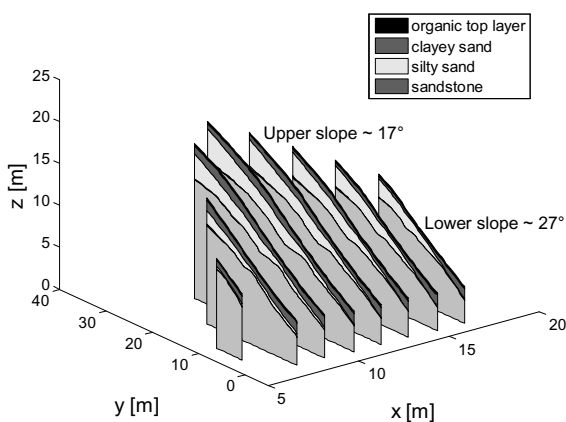


Figure 3. 3-dimensional model of the test site. The reference point of the model has the coordinates x, y, z = 0.

The first 7 soil samples have been taken using rammed samplers to investigate the soil structure and the layering of the topsoil. To carry out a soil classification after Swiss Standards (VSS, 1986, 1990a, 1991 and 1997), soil samples of more than two kilograms of material have been taken (for each depth) with a hand auger in boreholes at these 7 locations and at 6 other points.

It was impossible to reach the sandstone with the hand auger above 17 m reference height, because of water at a depth of circa 1m. The shallower slope angle of about 17° meant that a drilling apparatus could access the area and be operated successfully. Soil samples have been taken for classification and piezometers were installed in the same boreholes for later observation of the water level.

Classification was carried out following the Swiss Standards (VSS, 1997), based on USCS, including determination of the grain size distribution by sieving (VSS, 1986) and sedimentation (VSS, 1990a), determination of the density of solids (VSS, 1990b) and plasticity analyses (VSS, 1990c).

The sieve curves (Fig. 4) of all samples show that 50% percent of the soil fraction always exceeds a sieve size of 0.06 mm. So the official classification is, in all cases, a sand. Because the percentage of grains smaller than 0.06 mm is always over 12 %, plasticity analyses for the fine fraction were performed to distinguish between silty sand or tententially clayey silty sand (I_p of fines < 7%) and clayey sand (I_p of fines > 7%). Figure 4 shows all sieve curves grouped by their soil name. They range closely around the mean distribution of their group.

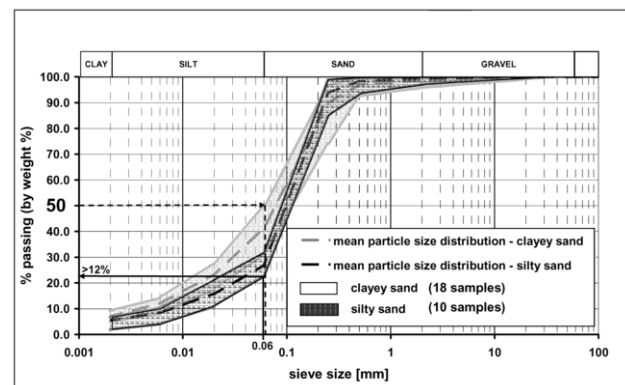


Figure 4. Sieve curves after Swiss Standard (VSS, 1986 and 1990a).

The results of the plasticity analysis are plotted in a diagram after the Swiss Standard (Fig. 5), classified by plasticity index against liquid limit. The fines of the soil samples belong to the groups CM, CL, which indicates a clayey sand or CL-ML and ML, which indicates a more silty to clayey and a silty sand.

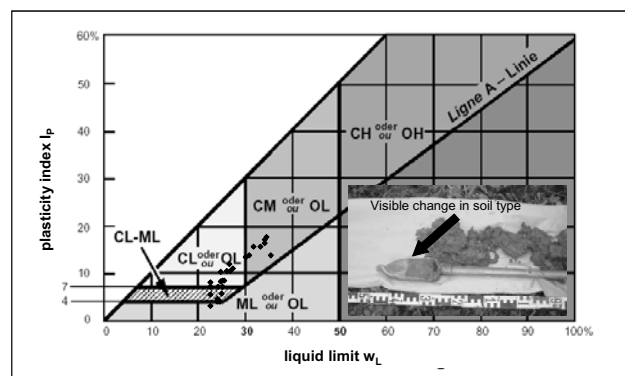


Figure 5. Results of the plasticity analysis and photo of one of the 21 samples. Diagram after Swiss Standards (VSS, 1997) based on USCS.

Photos from the field show sharp changes of soil colour indicating a change in soil type (Fig. 5) at depths that agree with the results from the laboratory tests (sieve and plasticity analysis). A 3-dimensional model of the test site area (Fig. 3) was constructed based on all results of the geotechnical investigations (Table 1).

Table 1: Depths of boreholes and location of the layering boundaries and depth of dynamic penetration tests (DPT).

bore-hole	Depth [m] of the layer			total depth [m]	DPT	total depth [m]
	hu-mus	clayey sand	silty sand			
1	0 - 0.2	0.2 - 1.6	1.6 - 2.0	2.0	1	0.9
2	0 - 0.4	0.4 - 1.6	-	1.6	2	3.4
3	0 - 0.3	0.3 - 1.3	1.3 - 1.7	1.7	3	3.6
4	0 - 0.3	0.3 - 1.3	1.3 - 1.8	1.8	4	4.1
5	0 - 0.3	0.3 - 0.9	0.9 - 1.2	1.2	5	0.9
6	0 - 0.3	0.3 - 0.8	0.8 - 1.0	1.0	6	2.3
7	0 - 0.3	0.3 - 0.9	0.9 - 1.0	1.0	7	2.3
8	0 - 0.3	0.3 - 0.7	0.7 - 1.3	1.3	8	2.3
9	0 - 0.3	-	0.3 - 1.8	1.8	9	0.8
10	0 - 0.3	0.3 - 1.3	-	1.3	10	0.8
11	0 - 0.3	0.3 - 1.0	-	1.0	11	1.3
12	0 - 0.3	0.3 - 1.5	-	1.5	12	1.5
13	0 - 0.3	0.3 - 0.8	0.8 - 1.3	1.3	13	0.6
A*	0 - 0.2	0.2 - 0.5	0.5 - 4.6	5.8		
B*	0 - 0.3	0.3 - 2.7	2.7 - 3.2	4.6		
		3.2 - 4.6				

* Borehole with drilling apparatus

An organic top layer of c. 30 cm overlay a layer of up to 1m thick clayey sand. The weathering product of the sandstone is the silty sand layer, which ranges from 10 to 60 cm deep in the lower part of the slope and becomes deeper at the top.

2.3 Geophysical investigation

Contrary to geotechnical testing methods, geophysical imaging techniques can be used to derive a spatial image of the subsurface in landslide or instable slope areas (e.g. Hack, 2000). An especially suitable parameter for landslide investigations is electrical resistivity ρ that increases with porosity Φ and saturation ratio S_r , following the relationship from Archie (1942).

$$\rho = \frac{a}{\Phi^m S_r^n} \rho_w \quad (1)$$

Here, a , m and n are empirical parameters and ρ_w is the water resistivity, which is relatively constant. Electrical resistivity is today most effectively mapped using electrical resistivity tomography (ERT). Recently successful applications for landslide investigation include the works of Suzuki and Higashi (2001) and Lapenna et al. (2003).

A complete 3D survey was performed on the test site employing altogether 15 profiles with 50 electrodes at 0.5 m spacings. Results of this 3D investigation comprising more than 12000 individual data points and an additional radar survey are described in detail in Friedel et al. (2005). Here, the focus is on individual 2D tomograms and comparison with the geotechnical model. Figure 6b shows a 2D resistivity model along profile EX08 produced from 3006 Wenner, Schlumberger and Dipole-Dipole measurements. Black colour represents low resistivity, and white indicates areas of high resistivity. The site can be divided into two parts. In the lower part, to $y = 12$ m, a layer of low saturation (white) overlies a thin layer of sediments with higher water content on top of the weathered sandstone, which is found at a depth of between 1 to 1.5 m. This is confirmed by the dynamic penetration tests DPT 12 and DPT 1.

In the upper part of the slope (beyond $y = 12$ m) the top of the sandstone dips away from the surface and is overlain by low resistivity material that is interpreted as quaternary deposits with higher content of fine material (silt, clay) and water-filled voids. The dip of the sandstone is confirmed by the greater depth of penetration of DPT 2 and DPT 3, though the latter test does not quite reach the depth predicted by the ERT image. In general, the high resolution ERT image detecting the discontinuity in layering in lower and upper parts of the slope proved to be very important for the later design of the monitoring system.

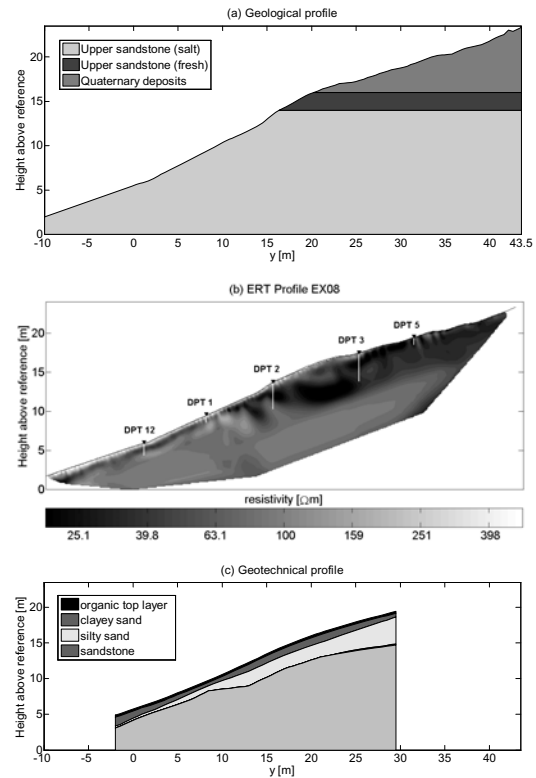


Figure 6. Comparison of results of geological (a), geophysical (b) and geotechnical investigations.

2.4 Influence of rainfall

One year after the initial resistivity survey in August 2003, the 2D ERT profiles were repeated in July 2004 to detect the influence of rainfall on the degree of saturation. Both years differ significantly in terms of the amount of precipitation. Rainfall in the months May to August amounted to [68, 41, 97, 76] mm in the comparatively dry summer of 2003, and [103, 75, 92, 88] mm in summer 2004. Figures 7a & b show the resistivity images of 2003 compared to 2004 in the most interesting lower part of the slope. The model from 2004 is based on 8071 measurements produced with 100 electrodes at 0.5 m spacings which was double the number of electrodes at the same spacing. While the general structure of the subsurface model with the parallel layering and the wedge shaped dip of the sandstone are found in both years, the low resistivity layer between the sandstone and the superficial layer is much more distinct in 2004 than in 2003.

The interpretation can be made solely in terms of saturation since all other parameters can be assumed to have remained constant. It follows, that major changes in water content occur in the layer on top of the sandstone. Another low resistivity anomaly at about 15 profile metres is also more distinct in 2004, indicating that water might accumulate in individual erosion features on top of the sandstone.

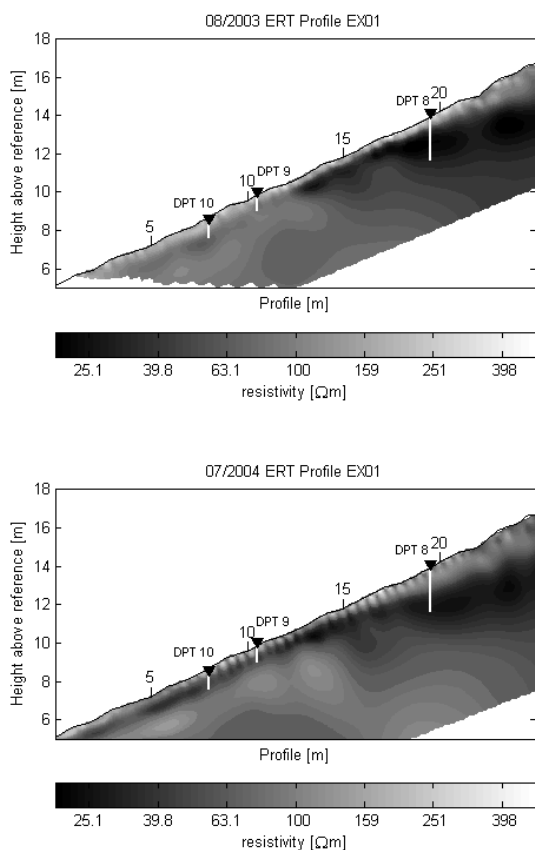


Figure 7. Comparison of resistivity tomograms (lower slope) taken in July 2003 and in August 2004. Profile metre is the unity of the length along the slope surface.

3 DISCUSSION AND CONCLUSION

In this study, a landslide endangered slope was investigated by combining the virtues of classical geotechnical testing (CGT) and electrical resistivity tomography (ERT). CGT allowed direct interpretation of grain size distribution and the plasticity index whereas the non-invasive and cost-efficient ERT delivered a high resolution spatial image of the subsurface in terms of resistivity. Furthermore, the disadvantages of CGT (invasive, time-consuming, only information at specific points or along few vertical profiles) and ERT (non-uniqueness of interpretation of resistivity in terms of soil type and parameters) could be reduced.

Both subsurface models produced by CGT and ERT show a high degree of similarity identifying a geological discontinuity along the slope, with a surface parallel layering in the lower part, and a thicker weathered layer covering a nearly horizontal sandstone surface in the upper part of the slope. Repeated ERT imaging also showed that major water content changes occur on top of the sandstone surface.

As a consequence of the combined investigation, the design of the monitoring experiment has been optimised. The majority of sensors (TDR, Tensiometers, Moisture Points) were installed in the lower part of the slope, where conditions are more uniform. Measurements commenced in July 2004.

ACKNOWLEDGEMENTS

Grateful thanks are due to Marco Sperl (IGT, ETH Zürich) who worked indefatigably on the field and carried out most of the laboratory classification tests.

We are also very grateful to Werner Attinger (ITÖ, ETH Zürich) for his assistance and helpful advices. René Rohr, Alfredo Privitello, Markus Iten, Thomas Weber, Matthias Preisig (IGT, ETHZ Zürich) and Felix Akeret were also enthusiastic fieldworkers at various times with the dynamic penetration tests and the geoelectrical investigation. Finally, with permission of the landowner (Mrs. Hiltbrand and Mr. Gehring) and the tenant farmer (Mr. Fritschi) we would not have been able to carry out this experiment. Their interest and support has been crucial.

REFERENCES

- Archie, G. E. 1942. The electrical resistivity log as an aid in determining some reservoir characteristics. *Trans. AIME* 146, 54-62.
- Bundesamt für Landestopographie 3084 Wabern, 1976. *Landeskarte der Schweiz 1:25000. Karte 1051 (Eglisau)*.
- ESI, Environmental sensors, 2004. homepage: <http://www.esica.com/products/moisture/index.html>
- Fischer, C.; López, J.; Springman, S.M. 2003. Remediation of an eroded steep slope in weathered sandstone after a major rainstorm. *International Conference on Landslides, Hong Kong, 8.-10. Dec. 2003*.
- Friedel, S. 2003. Resolution, stability and efficiency of resistivity tomography estimated from a generalized inverse approach. *Geophys. J. Int.* 153, 305-316.
- Friedel, S.; Thielen, A.; Springman, S.M. 2005. Investigation of a site endangered by rainfall-induced landslides using 3D resistivity tomography and geotechnical testing. *J. Appl. Geophys.* (submitted).
- Hack, R. 2000. Geophysics For Slope Stability. *Surv. in Geophys.* 21(4), 423-448.
- Hantke, R. 1967. *Geologische Karte des Kantons Zürich und seiner Nachbargebiete*. Kommissionsverlag Leemann, Zürich.
- Lapenna, V.; Lorenzo, P; Perrone, A.; Piscitelli, S.; Sdao, F; Rizzo, E. 2003. High-resolution geoelectrical tomographies in the study of Giarossa landslide (southern Italy). *Bull. Eng. Geol. and Env.* 62, 259-268.
- Suzuki, K.; Higashi, S. 2001. Groundwater flow after heavy rain in landslide-slope area from 2-D inversion of resistivity monitoring data. *Geophysics* 66(3), 733-743.
- University of Texas Libraries, 2000. political map of Switzerland (http://www.lib.utexas.edu/maps/europe/switzerland_pol_2000.jpg)
- VSS, 1986. *Mineralische Baustoffe und Lockergesteine – Siebanalyse*. Schweizer Norm SN 670810c.
- VSS, 1990a. *Mineralische Baustoffe, Schlammanalyse nach der Aräometermethode*. Schweizer Norm SN 670816a.
- VSS, 1990b. *Versuche: Dichte des Bodens*. Schweizer Norm SN 670335a.
- VSS, 1990c. *Konsistenzgrenzen*. Schweizer Norm SN 670345a.
- VSS, 1991. *Mineralische Baustoffe – Probenentnahme*. Schweizer Norm SN 670800c.
- VSS, 1997. *Identifikation der Lockergesteine – Labormethode mit Klassifikation nach USCS*. Schweizer Norm SN 670 008a.